

# Computational Solid Mechanics

## Assignment 1: Continuum Damage Modelling

Waleed Ahmad Mirza

### Abstract

The aim the project is to implement a Matlab algorithm to simulate damage modelling in isotropic materials. In physical terms damage occurs as a result of irreversible material degradation from processes involving initiation and growth of micro defects and as a consequence of which material suffers stiffness degradation. Damage is simulated for symmetric, tensile only and non-symmetric tension compression models under rate dependent(viscous) and rate independent (non-viscous) framework. Results have been validated using analytical model and intuitive interpretation.

### Part 1:Rate Independent framework

Mathematically, the term rate-independent is usually referred to time-dependent processes which are invariant under time rescaling. In physical term, in this framework, viscous behaviour of the material is ignored which decouples the stress generated in material to rate of deformation. In rate independent framework, following models are implemented in the formulated algorithm.

(a) Tension only and Non-symmetric models

In this section,a Matlab algorithm is formulated for simulating tensile only and non-symmetric tension compression model.In the provided pseudo Matlab code, commits are made in *dibujar-criterio-dano1.m*and *modelos-de-dano1.m* files as shown in Appendix A.1 and A.2.

(b) Linear and Exponential Hardening and Softening

In this section linear and exponential hardening ( $H > 0$ )/softening( $H < 0$ ) representing pure loading case is integrated in the formulated symmetric, tension only and non-symmetric damage models. For this purpose the provided Matlab file *rmap-dano.m* is modified as shown in Appendix A.3.

(c) Correctness of the Algorithm Implementation

The correctness and accuracy of implementation of damage model is gauged against a number of test cases involving various loading scenarios. The case studies are carried out using material properties mentioned in table 1.Note that in this analysis all physical parameters mentioned here are considered dimensionless.

Material Properties	Value
Young Modulus E	20000
Poisson Ratio $\nu$	0.3
Saturation value of hardening parameter $\sigma_{infinity}$	2
Hardening Modulus H	0.5
Yield strength $\sigma_y$	200
Viscosity $\eta$	0.5

Table 1 Material properties of employed in case studies

A simple case study is outlined here in order to establish the definition of the output parameter of the code. Fig.1 represents a case study when specimen is subjected to prescribed loads in terms of principle stress ( $\bar{\sigma}_1, \bar{\sigma}_2$ )loading path defined in time interval [0 10] i.e.(0, 0) $_{t=0} \rightarrow$  (300, 400) $_{t=3.333} \rightarrow$  (500, 400) $_{t=6.666} \rightarrow$  (500, 0) $_{t=10}$ . The path with red points on the plot illustrate the loading path in terms of effective principle stresses. While the path with black points represent the apparent stress ( $\sigma_1, \sigma_2$ ) generated in the specimen. It can be seen that in fig 1 apparent stress is always less than effective stress by a factor of (1-d) where d is the damage variable. And it can be noted that apparent stress and effective stress coincide as long as the material is in elastic range. As the loading exceed the yield strength  $\sigma_y$ , damage variable start playing a role in decreasing the load bearing strength of the material.

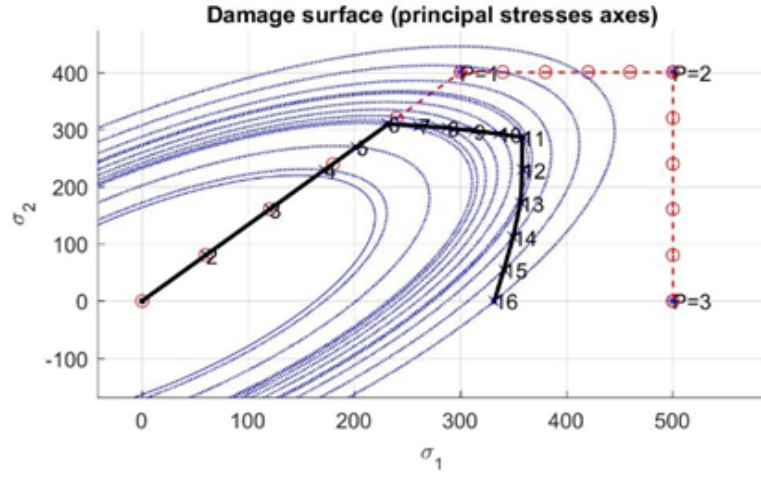


Figure 1 Zoomed in view of the damaged surface illustrating effective  $\bar{\sigma}$  (red) and apparent stress  $\sigma$  (black)

### 1-Test Case 1

In this case study a loading path involving uni-axial tensile and compressive load is applied on the specimen as show as follow:

$$\begin{cases} \Delta\bar{\sigma}_1^{(1)} = 500; \Delta\bar{\sigma}_2^{(1)} = 0; \\ \Delta\bar{\sigma}_1^{(2)} = -600; \Delta\bar{\sigma}_2^{(2)} = 0 \\ \Delta\bar{\sigma}_1^{(3)} = 600; \Delta\bar{\sigma}_2^{(3)} = 0 \end{cases}$$

Under loading conditions prescribed above, a number of plots are generated with the formulated algorithm. Results are presented in terms of evolution of internal variable  $r$  and stress-strain plot. Results of each model are discussed one by one as follow:

**Symmetric Tension Compression model:** For symmetric model (fig. 2), in first phase of loading, the material behaves linear under yield strength but as the loading exceeds the yield strength, the curve exhibit nonlinear behaviour as material stiffness starts to degrade. Moreover as material damage under pure loading scenario, .the damage surface start to expand due to hardening of material. From  $P_1$  to  $P_2$  the loading curve changes its direction and the material is subjected to compression state. The point to be noted here is that under compression the material curve restores back with a different slope. Under compression the material behaves linearly as long as the apparent stresses are within the damage surface and then changes its slope as material starts to damage. This trend can be verified in stress-strain plot in fig. 3.

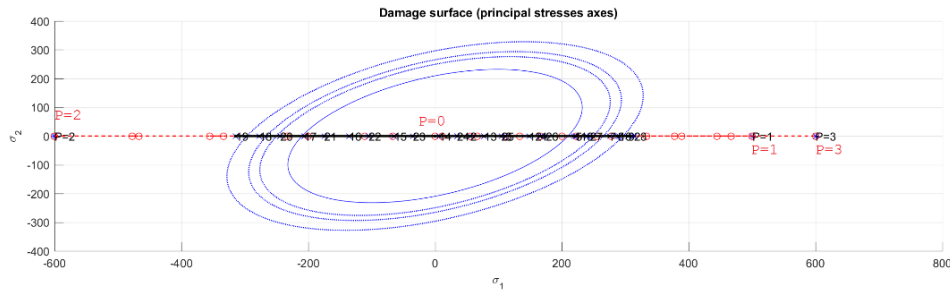


Figure 2 Symmetric model Damage surface

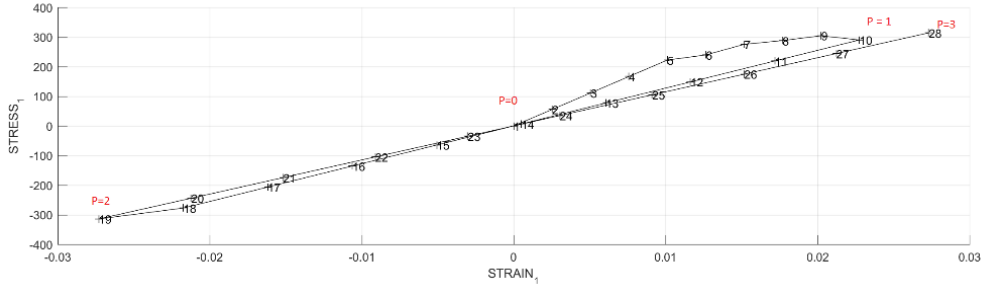


Figure 3 Symmetric model: Stress-Strain plot

In internal variable  $r$  evolution plot (fig 4), it can be seen that  $r \geq 0$  and it stays constant in the elastic range and increase its value as material cross nonlinear range. Moreover from the internal variable evolution plot it can be seen that:

$$\frac{TensileLoad}{CompressiveLoad} = \frac{500}{600} \sim \frac{Max.raftertension}{Max.raftercompression} = \frac{3.20}{3.75}$$

~ 1

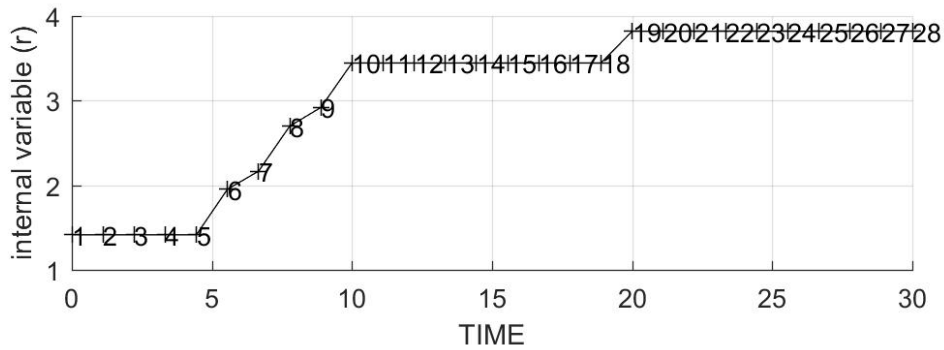


Figure 4 Symmetric model: Internal variable evolution

**Tension-only model:** In tensile only model, the material undergo nonlinearity in tensile phase (P=0 to P=1) and yields exactly the same results as in symmetric model but in compression phase (P=1 to P=2) material does not undergo degradation and from P2 to P3 the stress strain curve returns with the same value of slope as from P1 to P2 and the internal variable  $r$  does not evolve under compression. Results of tension only model are illustrated in fig 5, 6 and 7.

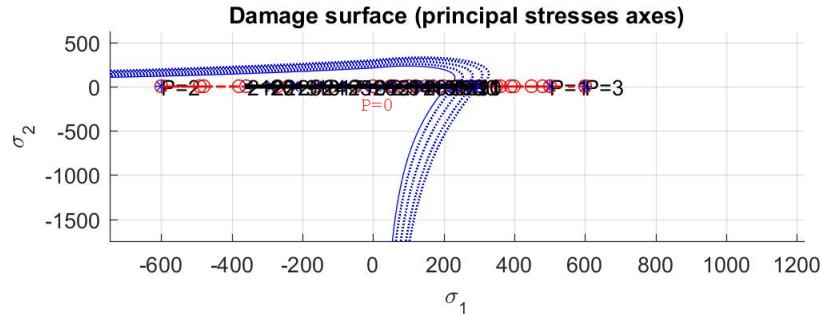


Figure 5 Tension only model Damage surface plot

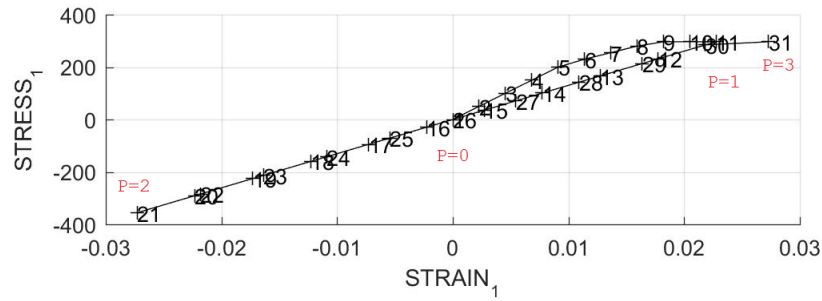


Figure 6 Tension only model: stress-strain plot

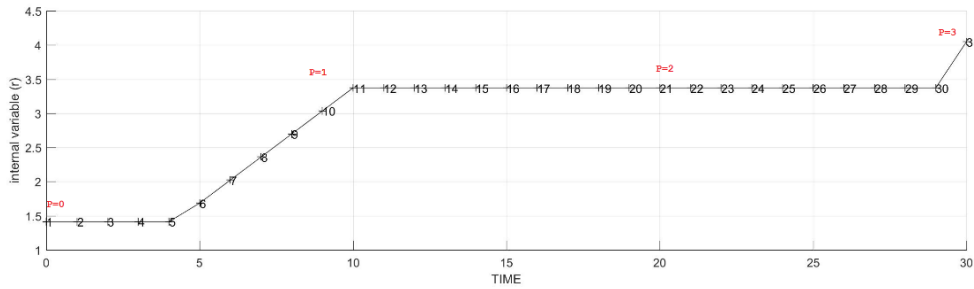


Figure 7 Tension only model: Internal variable evolution plot

**Non symmetric Tension Compression model:** In the non-symmetrical model, value of  $n$  is set equal 3 that physically implies that compressive strength of the material is three times higher than the symmetric case but not infinitely high as the tension-only model. In this case, that material damage in compression but the non-linear stress strain curve start when stress exceed almost the three times of the yield strength value. Hence nonlinearity representing damage in material is less as compared to the symmetric model. But in the presented test case, the prescribed loading does not exceed the material compressive yield strength. Therefore there is no non-linearity in compression. Moreover the damage variable  $d$  or the internal variable  $r$  only evolve in inelastic regime. Therefore these parameters don't evolve in compression (P=1 to P=2) and only evolve in tension phase (P=0 to P=1 and P=2 to P=3). The results of this model are described in fig. 8,9 and 10.

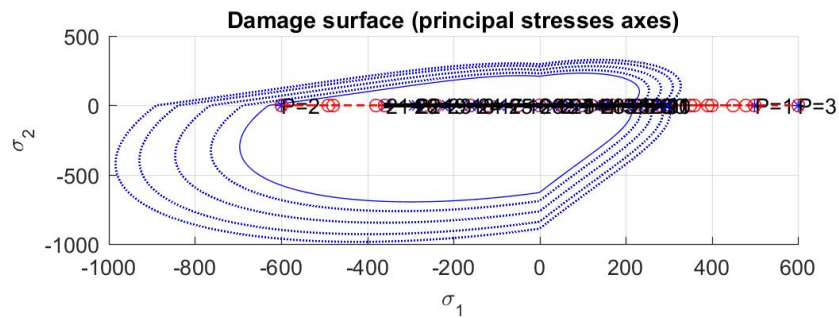


Figure 8 Unsymmetrical Tension Compression model: Damage surface plot

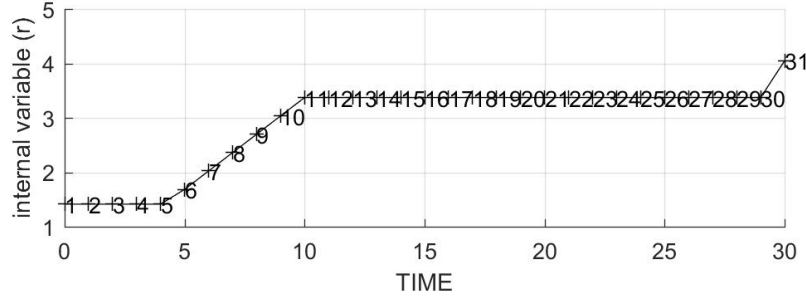


Figure 9 Unsymmetrical Tension Compression model: Evolution of internal variable r

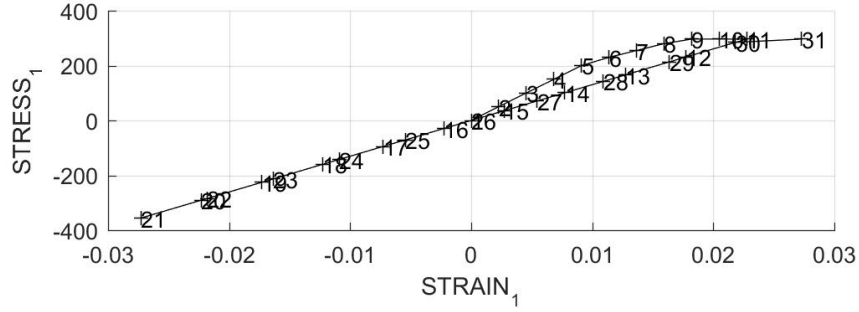


Figure 10 Unsymmetrical Tension Compression model: Stress Strain plot

## 2-Test Case 2

The given prescribe loading conditions involve one uniaxial load and two biaxial loads. For each damage model, the results are analysed using damage surface plot and stress-strain plots.

$$\begin{cases} \Delta \bar{\sigma}_1^{(1)} = 500; \Delta \bar{\sigma}_2^{(1)} = 0; \\ \Delta \bar{\sigma}_1^{(2)} = -600; \Delta \bar{\sigma}_2^{(2)} = -600 \\ \Delta \bar{\sigma}_1^{(3)} = 700; \Delta \bar{\sigma}_2^{(3)} = 700 \end{cases}$$

**Symmetric Tension Compression model:** In symmetric model in first phase of the plot (fig.11 and 12) from point P=0 to P=1, the material undergo a tensile test. The results obtained for this phase are quite similar to test case study 1 where the material start to degenerate as soon as loading exceeds the yield strength of the material. The second and third phase, from point P=1 to P=3, the material undergo damage both in compression and tension as can be seen in stress-strain plot in fig.11. This trend can be confirmed from evolution of internal variable r in fig. 12, where there is a slight fluctuation from point P=1 to P=2 and then just before P=3.

**Tension Only model:** In tension only model, the material behaves very similar to the symmetric case under uniaxial loading. From P=1 to P=2, under compression the material remains linear as can be seen in figure 13 There is no evolution in damage variable d or internal variable r. As the curve move toward from P=2 to P=3 the damage surface start to expand again as internal variable r start evolving again as can be seen in fig 14.

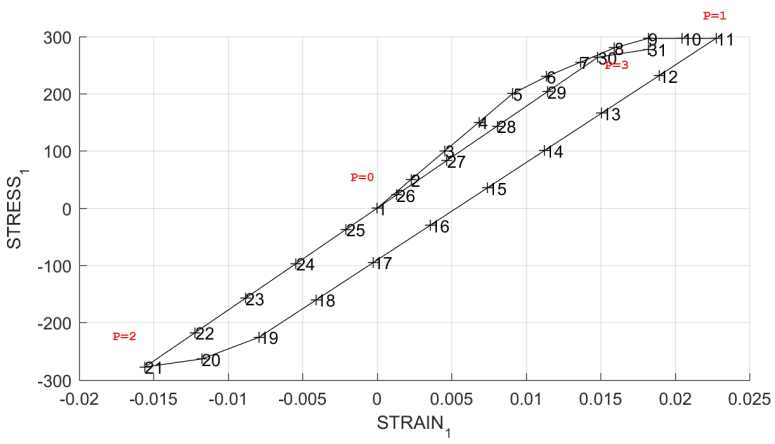
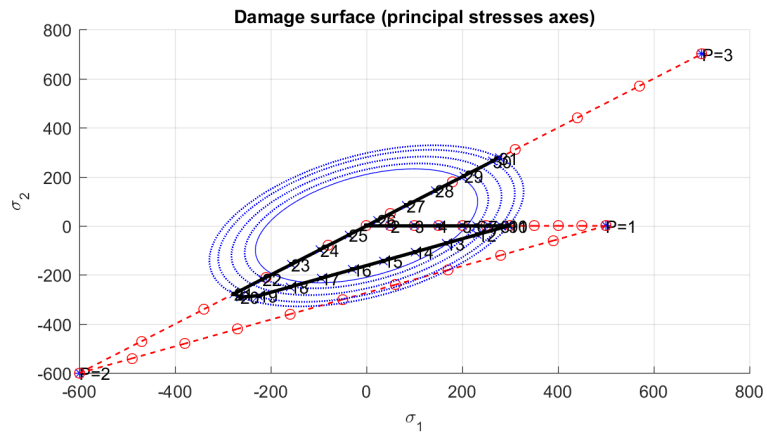


Figure 11 Results of Symmetric model a)Damage surface plot(Top)b)Stress-strain plot(Bottom)

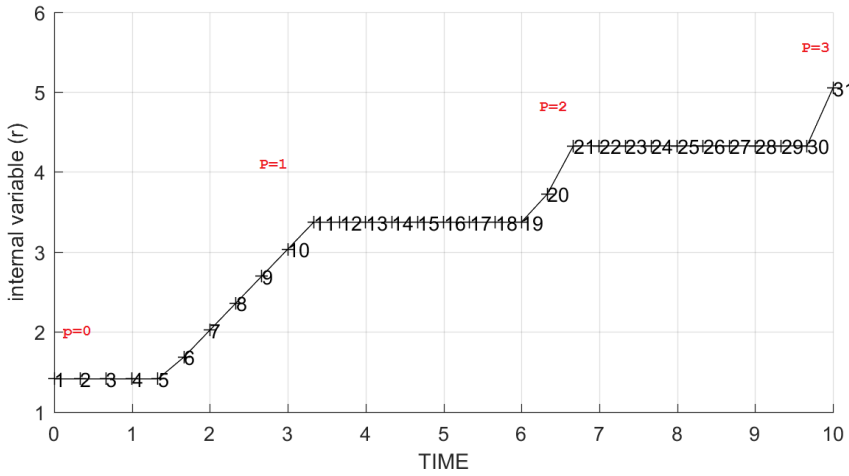


Figure 12 Symmetric model: Internal variable plot

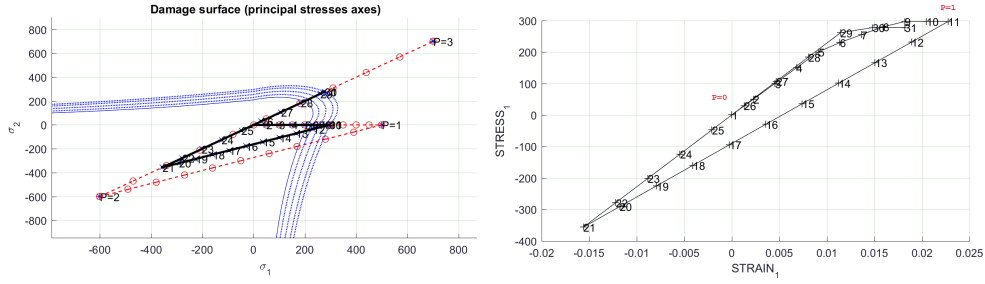


Figure 13 Tension only model: a) Damage surface plot(right) b) Stress-strain plot(left)

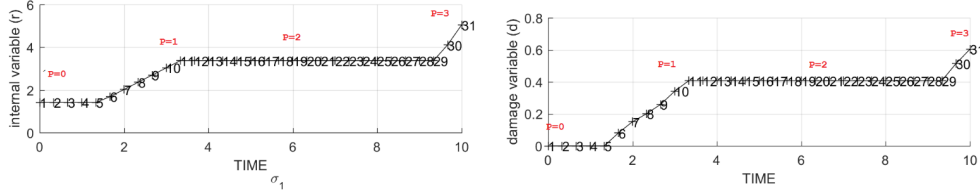


Figure 14 Tension only model: Evolution of internal variable  $r$ (left) and damage variable  $d$ (right)

**Non symmetric Tension Compression model:**For tension compression model, the plots are illustrated in fig.15. It can be seen that the plot is exactly similar to symmetric case for phase 1 and phase 3. In phase two, the plot, due to high compression yield strength, the material behaves linear and there is no evolution in damage variable  $d$  or internal variable  $r$ .

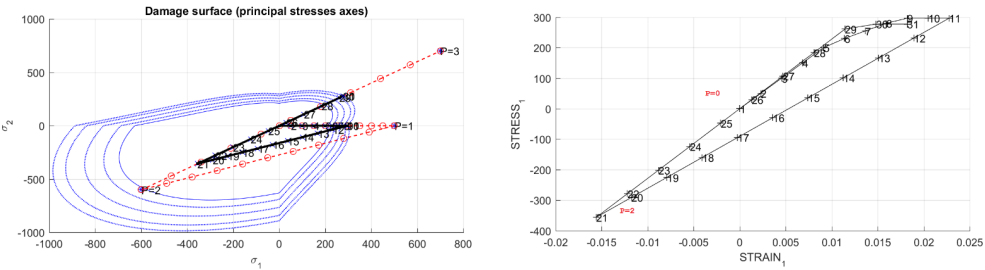


Figure 15 Non-symmetric Tension Compression model a) Damage surface plot(left) b) Stress-strain plot(right)

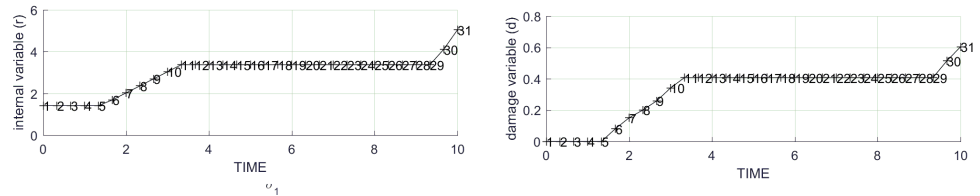


Figure 16 Non Symmetric Tension Compression model: Evolution of internal variable  $r$ (left) and damage variable  $d$ (right) in time

### 3-Test Case 3

Case study 3 consist of three biaxial loads such that in each loading steps the magnitude of loading is greater than the previous step as follow:

$$\begin{cases} \Delta\bar{\sigma}_1^{(1)} = 500; \Delta\bar{\sigma}_2^{(1)} = 500; \\ \Delta\bar{\sigma}_1^{(2)} = -600; \Delta\bar{\sigma}_2^{(2)} = -600 \\ \Delta\bar{\sigma}_1^{(3)} = 700; \Delta\bar{\sigma}_2^{(3)} = 700 \end{cases}$$

**Symmetric Tension Compression model:** For symmetric case, the damage surface and stress strain curve are illustrated in fig 17. It can be seen that in damage surface plots, the trend observed in first phase of biaxial loading from  $P=0$  to  $P=1$ , is very similar to test case study 2. Nonlinearity is observed in this phase as loading exceeds the materials yield strength. Similarly nonlinearity is observed in other two phases of the loading as well for the similar reasons. Moreover in the fig. 18 it can be seen that the value of damage variable  $d$  or internal variable  $r$  increases by end of every loading phases.

**Tension only model:** For tension only case the results are displayed in fig 19 and 20. In figure, the curve undergo non-linearity twice: once in first phase (from  $P=0$  to  $P=1$ ) and second time in third phase (from point  $P=2$  to  $P=3$ ) as can be verified from the internal variable  $r$  vs time plot.

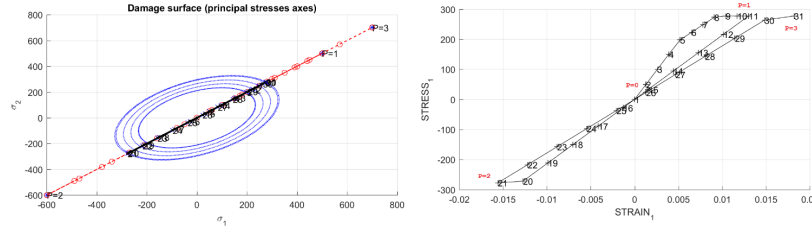


Figure 17 Symmetric model: damage plot surface(left), stress-strain plot(right)

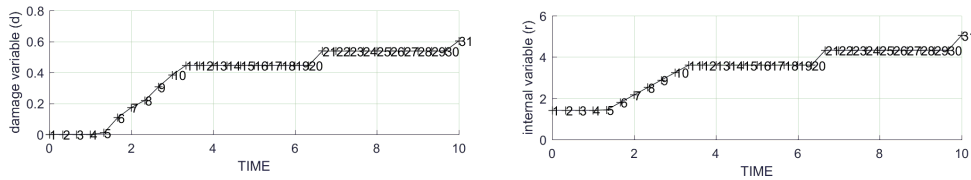


Figure 18 Symmetric model: Internal variable evolution(right) damage variable evolution(left)

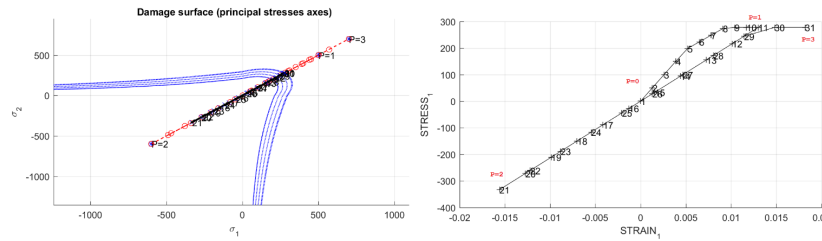


Figure 19(a) Tension only model: a) Damage surface(left) b) Stress-strain plot(right)

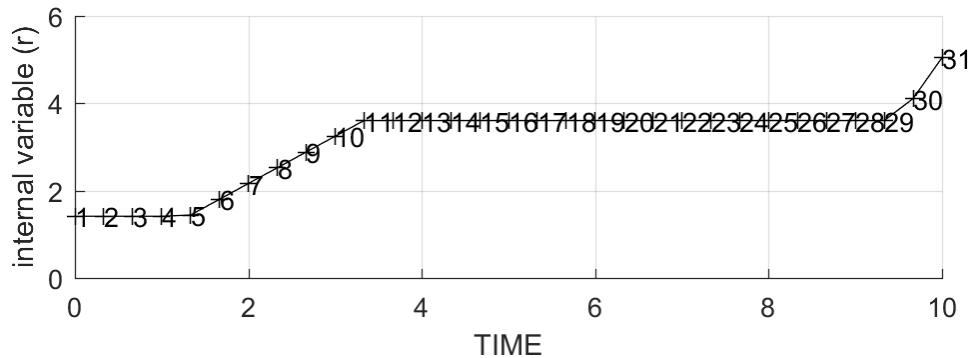


Figure 20 Tension only model: Evolution of internal variable  $r$

For tension compression case the results are plotted in fig 21 it can be seen that the damage surface does not only evolves in biaxial tension tests i.e. in phase 1 and 3 as the loading in the material does not exceed the yield strength and behaves elastic. This trend can be verified by can be verified from the internal variable  $r$  vs time plot as can be seen in fig. 22.



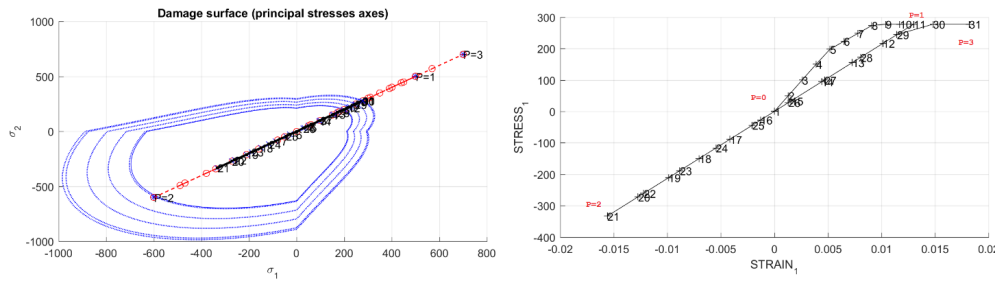


Figure 21 Un-symmetric model: Damage surface plot(left)-stress strain plot(right)

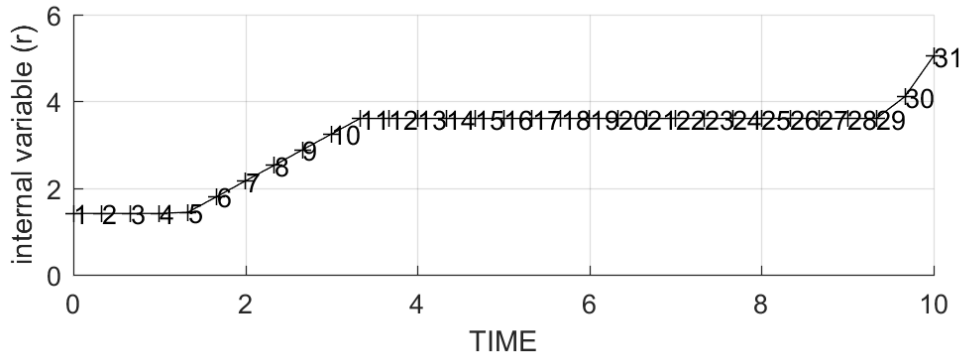


Figure 22 Un-symmetric tension compression model: Internal variable evolution

#### 4-Verification of implementation of exponential hardening

Exponential hardening and softening model is implemented in the formulated Matlab code as shown in appendix A.3. Hardening and softening trends have been analysed for a uniaxial case study involving prescribe loading data of test case study 1.

Hardening is studied for a range of values of  $H$  as shown in figure 23. It should be noted that here the value of  $q_{infinity}$  is set to be 2. Results are studied in terms of various plots as illustrated in fig.23. Softening in the material is studied setting values of  $q_{infinity}$  to be  $10^{-6}r_0$ . Value of  $q_{infinity}$  is not set zero for numerical stability of the code. Note that in hardening variable  $q$  vs time plot the curve shifts up as hardening modulus is increased as shown in figure 21. Moreover  $q$ - $r$  plot behaves as expected and does not go beyond  $q_{infinity}$ .

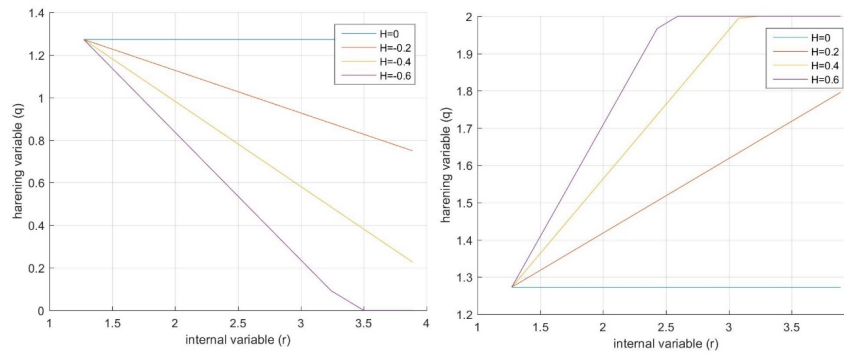


Figure 23 Linear hardening model: Hardening variable vs internal variable plot for a) Softening ( $H < 0$ ) b) Hardening ( $H > 0$ )

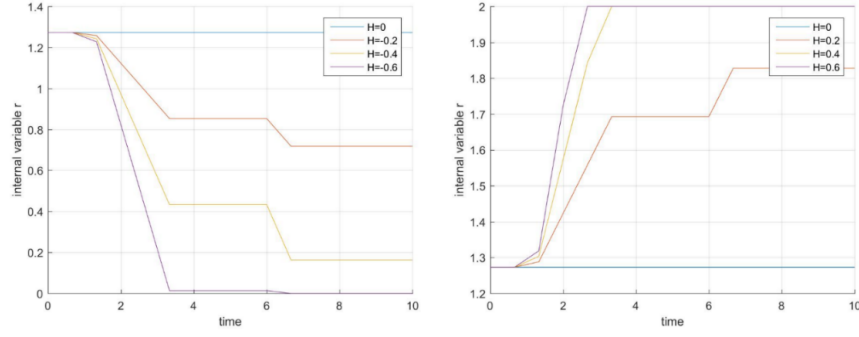


Figure 24 Linear hardening model:Internal variable evolution plot for various values of hardening modulus  $H$

The exponential hardening and softening have been plotted in figure 25. The hardening and softening have been studied for varying values of  $A$ . For softening, the  $q_{inf}$  was set at  $10^{-6}r_0$ . The curves behave as expected, and developed faster with higher values of  $A$ .

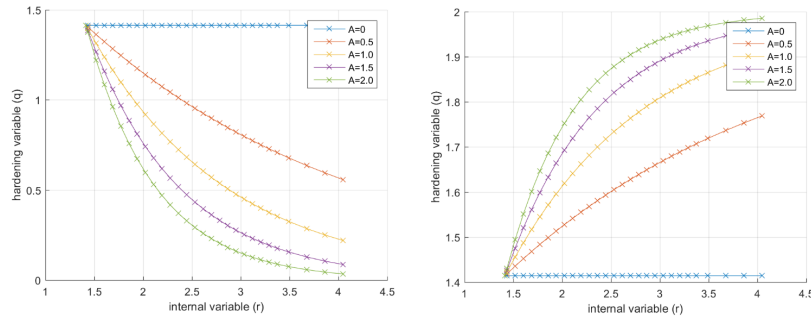


Figure 25 Exponential hardening model:Hardening variable vs internal variable plot a)Softening ( $H < 0$ )b)Hardening ( $H > 0$ )

## Part 2:Rate Dependent models

### 1. Implementation of rate dependent model

Rate dependent model is implemented in the formulated Matlab algorithm for symmetric compression tension model. Details of the changes committed in the provided pseudo code are given in Appendix B.1.

To verify the trends of the obtained plot, the formulated algorithm is implemented for a case study using the input data given in table 1. The damage surface obtained for this case study is illustrated in fig. 26. It can be seen that unlike in inviscid model, this case the apparent stress points(black) can lie outside the damage surface.

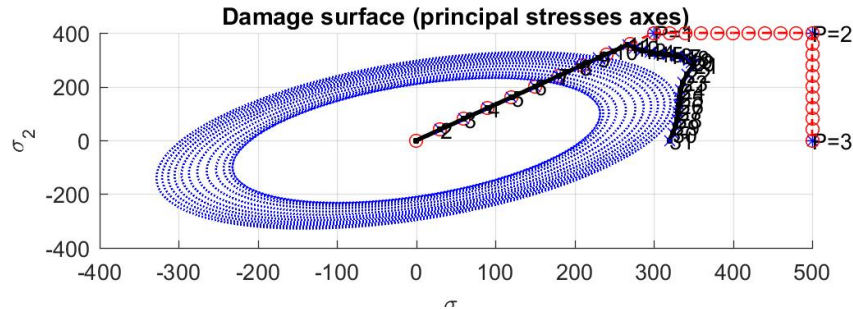


Figure 26 Rate dependent mode Damaged surface at  $\Delta t = 0.1$  illustrating effective  $\bar{\sigma}$  (red) and apparent stress  $\sigma$  (black)

### 2. Verification of implementation of rate dependent model

In this section the influence of input parameters like viscosity  $\eta$ , strain rate  $\dot{\epsilon}$  and on stress-strain plot is studied using the formulated algorithm and results are compared with analytical model to establish the accuracy of algorithm. **Note that material parameters are adopted from table 1 and value of  $\alpha$  is set to 0.5.**

(a) **Viscosity  $\eta$**

Influence of value viscosity on stress-strain plot are analysed for a uniaxial test with loading conditions:

$$\Delta\bar{\sigma}_1^{(1)} = 1000; \Delta\bar{\sigma}_2^{(1)} = 0; \quad (1)$$

It can be seen in fig. 27 that as increasing viscosity value shifts the stress-strain plot upward i.e. it increases the value of apparent stress in the material.

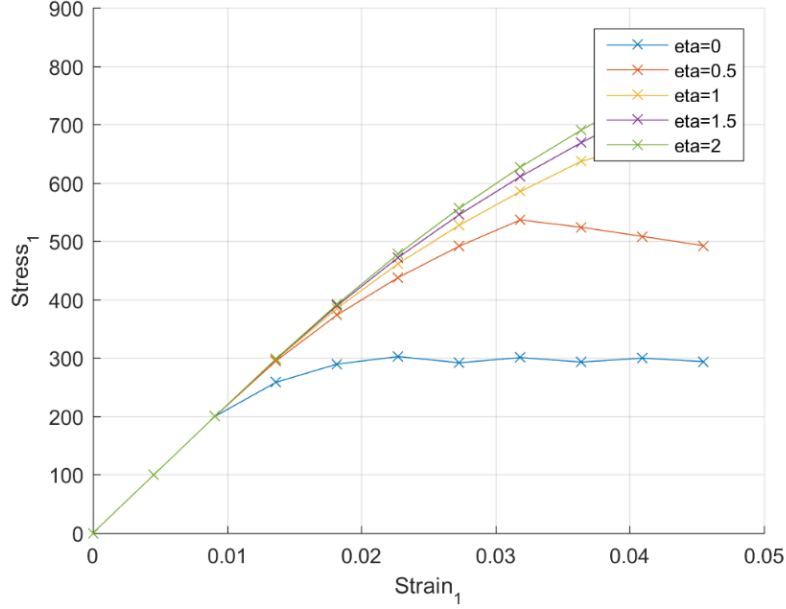


Figure 27 Influence of viscosity at  $\Delta t = 0.1$

Moreover the value of damage variable decreases with increasing viscosity as shown in fig 28.

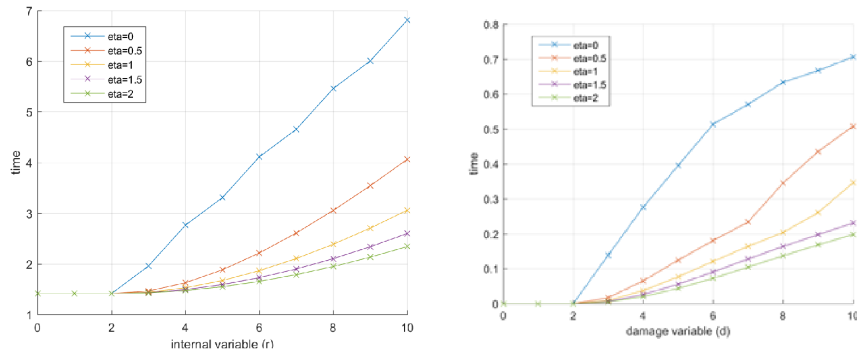


Figure 28 Influence of internal variable for  $\Delta t = 0.1$ (left)and damage variable ( $d$ )(right)

This result is consistent with the analytical model [1] i.e.

$$\sigma(t, \epsilon(t)) = (1 - d(r(t)))C : \epsilon \quad (2)$$

$$d = 1 - \frac{q}{r} \quad (3)$$

As  $r$  decreases with increasing viscosity  $\eta$ , as a consequence  $d$  decreases which according to equation 2 increases the value of apparent stress.

(b) **Strain rate  $\dot{\epsilon}$**

Fig.29 shows the damage surface plot of the presented case study at  $\Delta t = 100$  and  $\Delta t = 0.001$ . It should be noted that

less value of  $\Delta t$  reflect a higher strain rate. Hence from fig. 29 it can be seen that a higher apparent stress is obtained at a high strain rate as in general for rate dependent model stress is directly proportional to the strain rate. Hence higher the strain rate, higher would be the apparent stress. This result is also obvious in the stress-strain plot depicted in fig. 30.

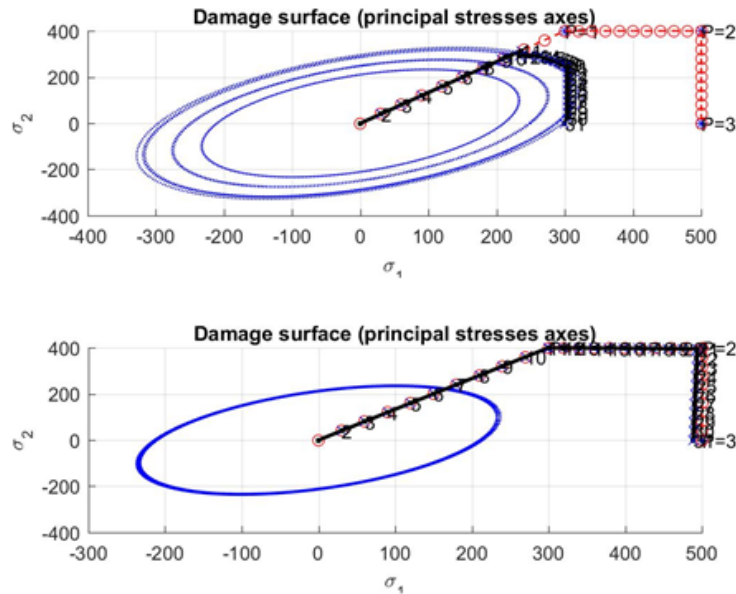


Figure 29 Damage surface models for  $\Delta t = 100$ (left) and  $\Delta t = 0.001$ (right)

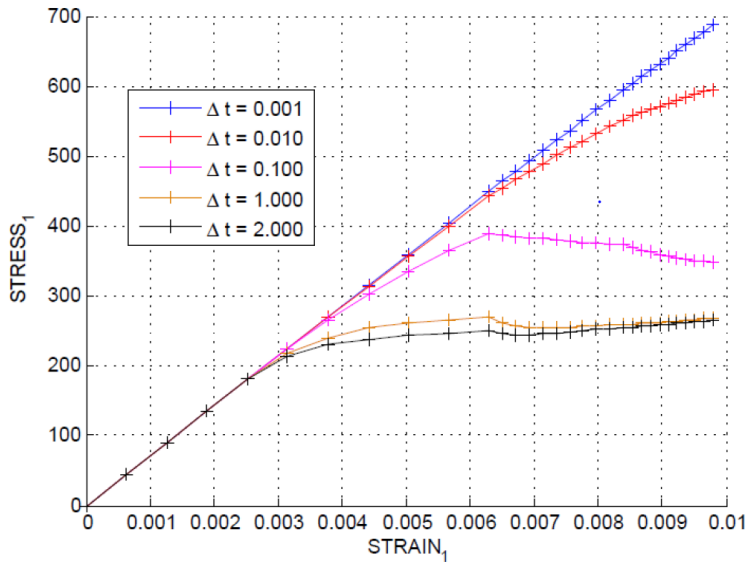


Figure 30 Influence of varying values of  $\Delta t$  on stress-strain plot)

(c) **Alpha  $\alpha$**

The value of alpha  $\alpha$  influences the stability of results. Each value of alpha correspond to a different method as described follows:

- (a) For value of  $\alpha = 0$ , the method corresponds to Backward Euler (Explicit) time integration method. This method is first order accurate in time  $O(\Delta t)$ . This method is fast but less robust.
- (b) For value of  $\alpha = 1.0$ , the method corresponds to Forward Euler( Implicit)time integration method. This method is first order accurate in time and space  $O(\Delta t)$ . This method is robust compared to Backward Euler method.

- (c) For value of  $\alpha = 0.5$ , the method corresponds to Crank Nicolson time integration method. This method is second order accurate in time and space  $O(\Delta t^2)$ . This method is the most robust and accurate compared to the former two method.

In the following test stress-strain curve of a uniaxial test is evaluated for varying values of  $\alpha$  at  $\Delta t = 10$ . Fig.31 presents result of the test and it can be seen that stress-strain plot for  $\alpha = [0.5, 1]$  give least oscillation while  $\alpha = 0$  give most oscillations. This proves that time integration is only unconditionally stable for value  $\alpha = [0.5, 1]$ .

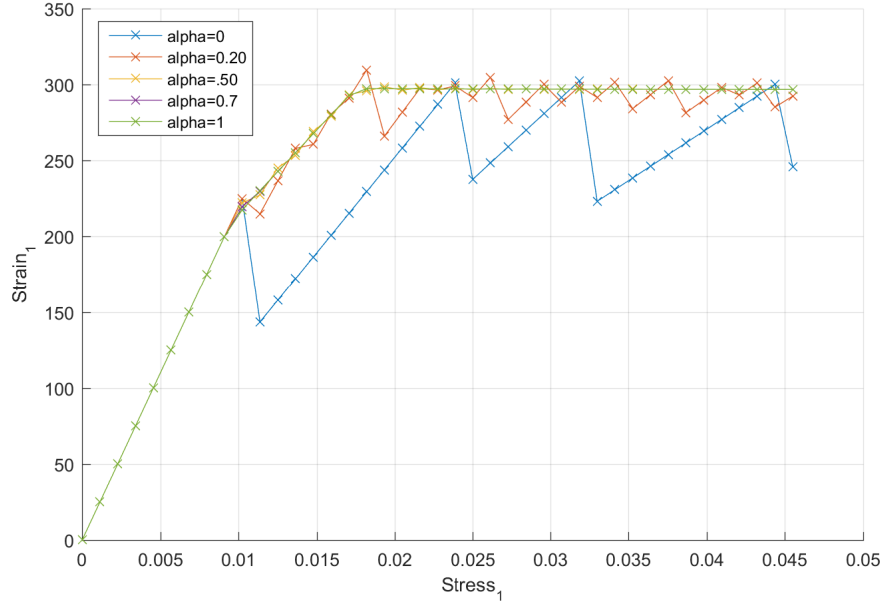


Figure 31 Influence on stress-strain curve for varying values of  $\alpha$

In the literature [1] it can be seen that numerical integration dont propagate error for values of  $\Delta t$  such that

$$-1 \leq \frac{[\eta - \Delta t(1 - \alpha)]}{\eta + \alpha \Delta t} \leq 1 \quad (4)$$

Following equation 4 for the value of  $\Delta t$  for which stable integration is obtained is  $[0, 2\eta]$ . For  $\eta = 0.5$  the result obtained is depicted in fig.32.

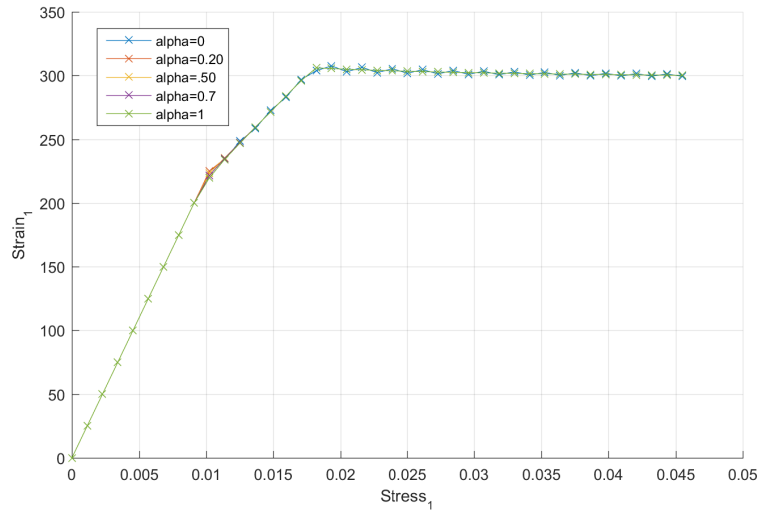


Figure 32 Influence on stress-strain curve for varying values of  $\alpha$  at  $\Delta t = 1$

It can be seen that for  $\alpha = 0$ , the plot shows some initial fluctuations, but the fluctuations dont propagate and diminish with time.

(d) **Comparison of  $C_{11}$  with  $\alpha$  values**

The algorithmic  $C_{11}^{alg}$  and secant tangent operator  $C_{11}^{tangent}$  at is implemented in the formulated algorithm as shown in appendix B.2. The evolution of  $C_{11}$  element of consistent algorithmic and tangent operator is analysed for varying values of  $\alpha$  as shown in fig 33. The test has been conducted for the values of loading conditions of test case study 1. The value of  $\Delta t$  and  $\eta$  is set to be 1 and 2 respectively. It can be seen that value of  $C_{11}^{alg}$  and  $C_{11}^{tangent}$  increases with increasing  $\alpha$  values.

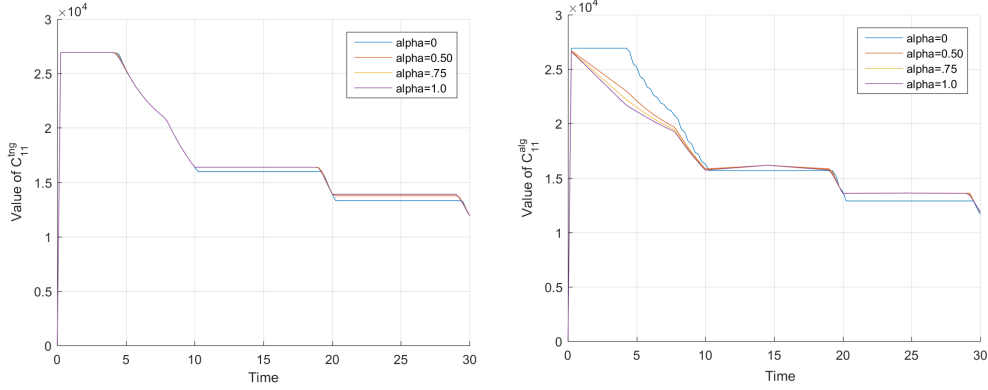


Figure 33 Evolution of  $C_{11}^{tangent}$  and  $C_{11}^{alg}$  with varying  $\alpha$

Moreover for  $\alpha = 0$ ,  $C_{11}^{tangent}$  and  $C_{11}^{alg}$  give the same value in time and for rest of the values of  $\alpha$   $C_{11}^{tangent}$  is always greater than  $C_{11}^{alg}$  as shown in fig 34.

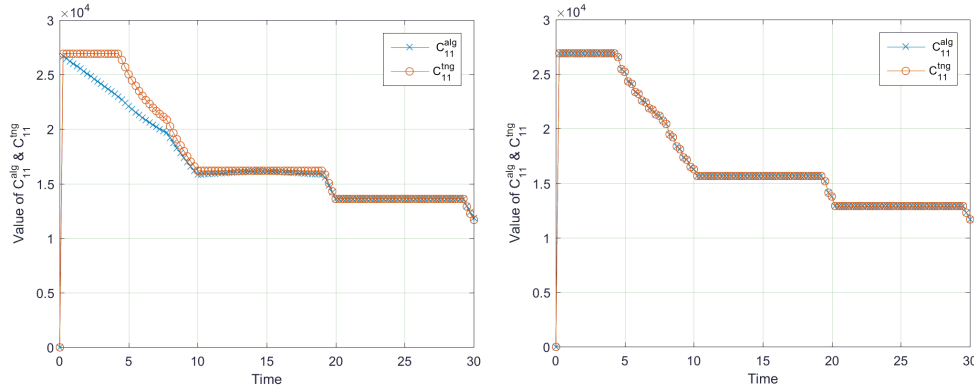


Figure 34 Evolution of  $C_{11}^{tangent}$  and  $C_{11}^{alg}$  at  $\alpha = 0.5$ (left)and at  $\alpha = 0$ (right)

This behaviour of  $C_{11}^{tangent}$  and  $C_{11}^{alg}$  is consistent with analytical model presented in literature[1].

## Discussion and Conclusion

In this study an algorithm is formulated to implement damage modelling in isotropic materials. The algorithm has been tested for a number of case studies under rate independent (non-viscous) and rate independent (viscous) framework involving uniaxial and biaxial tension/ compression loading paths. Following conclusions have been obtained from the analysis of case studies in rate independent framework.

1. The material behaves perfectly elastic under neutral loading and unloading.
2. A soon as the apparent stress load tries to jump out of the damage surface under pure loading, the surface expands and parameters like internal variable  $r$  and damage variable  $d$  increase. In such phase the material undergo decrease in stiffness.
3. In tensile strength model material is only able to undergo nonlinearity in tensile phase whereas in compression, the material does not undergo damage.

4. In non-symmetric tension compression model (for  $n > 1$ ), the material is more resilient to damage under compressive load compared to the symmetric model.

From analysis of case studies in rate dependent model, following conclusions are derived.

1. With increasing viscosity, the apparent stress in the material increases.
2. Increasing the strain rate increases the apparent stress magnitude in the materials.
3. C11 component of algorithmic and tangential stiffness matrix give the same value for  $\alpha = 0$ . Apart from that for other values of  $\alpha$ , the C11 component of tangential stiffness matrix is always equal to or greater than the algorithmic stiffness matrix.
4. For values of  $\alpha = 0 \in [0.5, 1]$  numerical time integration give stable and accurate results.

## References

- 1) Xavier Oliver (2016), 'Lecture 4 and 5: Damage modelling', Polytechnic University of Catalonia.

## Appendix

### A Rate Independent model

#### A.1 Tension only model

```
% Following changes are made in dibjur_criterio_dano1.m
if MDtype==2

    tetha=[0:0.01:2*pi];
    %*****
    %* RADIUS
    D=size(tetha);          %* Range
    m1=cos(tetha);          %*
    m2=sin(tetha);          %*
    Contador=D(1,2);        %*
    radio = zeros(1,Contador) ;
    s1     = zeros(1,Contador) ;          %First Principle Stress
    s2     = zeros(1,Contador) ;          %Second Principle Stress
    for i=1:Contador
        sigma =([ m1(i) m2(i) 0 nu *( m1(i)+m2(i))]);
        sigma_plus =( sigma + abs ( sigma ) ) /2; % The Macaulay bracket of stress tensor
        radio (i)= q/ sqrt ( ( sigma_plus ) * ce_inv * [ m1(i) m2(i) 0 nu *( m1(i)+m2(i)) ]');
        s1(i)=radio(i)*m1(i);
        s2(i)=radio(i)*m2(i);
    end
    hplot =plot(s1,s2,tipo_linea);
end
```

```
% following are the changes made in Modelos_de_dano1.m
elseif (MDtype==2)
    new_sigma = ce* eps_n1';
    new_sigma_plus = ( abs ( new_sigma )+ new_sigma ) /2;% Calculate <Sigma >
    rtrial = sqrt ( eps_n1 * new_sigma_plus ); % Calculate strain norm
```

#### A.2 Non symmetric model

```
% following are the changes made in Modelos_de_dano1.m
elseif (MDtype==3)          % For Non-symmetric model
    new_sigma = ce* eps_n1'; % Calculate stress
    new_sigma_plus = ( abs ( new_sigma )+ new_sigma ) /2; % Calculate <Sigma >
    theta = sum ( new_sigma_plus ) / sum ( abs ( new_sigma_plus ) ); % Calculate theta
    rtrial= (theta+(1-theta)/n)*sqrt(eps_n1*ce*eps_n1') ;
end
```

```
%This part is implemented in dijbujaar_criterio_dano1.m
if MDtype==3
    tetha=[0:0.01:2*pi];
    %*****
    %* RADIUS
    D=size(tetha);          %* Range
    m1=cos(tetha);          %*
    m2=sin(tetha);          %*
    Contador=D(1,2);        %*

    radio = zeros(1,Contador) ;
    s1     = zeros(1,Contador) ;
    s2     = zeros(1,Contador) ;

    for i=1:Contador
        sigma_macaulay =( m1(i)+m2(i) + abs (m1(i))+ abs(m2(i))) /2; % Numerator of theta
        sigma_absolute = abs(m1(i))+ abs (m2(i) ); % Denominator of theta
        theta = sigma_macaulay / sigma_absolute ; % Calculation of theta
        radio (i) = ((1) / ( theta +(1 - theta ) / (n) )) * (q/ sqrt ( [ m1(i) m2(i) 0 nu *( m1(i)+m2(i) ) ] *...
            ce_inv * [ m1(i) m2(i) 0 nu *( m1(i) +m2(i) ) ]' ));
        s1(i)=radio(i)*m1(i);
        s2(i)=radio(i)*m2(i);
    end
    hplot =plot(s1,s2,tipo_linea);
end
```



### A.3 Hardening/Softening Implementation

```

% following a re the changes made in rmap_dano1.m
if(rtrial > r_n)
    %* Loading
    fload=1;
    if Eprop (6) ==1 && MDtype ==1 % Viscous case and symmetric model
        r_n1 =((eta-delta_t*(1 - alpha ))*r_n+( delta_t*rtrial ) ) /( eta+alpha*delta_t );
    else
        r_n1 = rtrial;
    end
    delta_r=r_n1-r0;
    if hard_type == 0

        if sign(H) == -1.0 % setting value of q_infinity for softening
            q_inf = zero_q;
        end
        % Linear Hardening
        r1=r0 +( q_inf -r0)/H;
        if r_n1 <r1

            q_n1= r0+ H*delta_r;
        else
            q_n1 = q_inf ;
        end
    else
        if sign(H) == -1.0 % setting value of q_infinity for softening
            q_inf = zero_q ;
        end
        q_n1 = q_inf-(q_inf-r0)*exp(A*(1-r_n1/r0));
    end
    if(q_n1<zero_q)
        q_n1=zero_q;
    end
end

```

```

%This part is implemented in dijbujar_criterio_dano1.m
if MDtype==3
    tetha=[0:0.01:2*pi];
    %*****
    %* RADIUS
    D=size(tetha); %* Range
    m1=cos(tetha); %*
    m2=sin(tetha); %*
    Contador=D(1,2); %*

    radio = zeros(1,Contador) ;
    s1 = zeros(1,Contador) ;
    s2 = zeros(1,Contador) ;

    for i=1:Contador
        sigma_macaulay = ( m1(i)+m2(i) + abs (m1(i))+ abs(m2(i))) /2; % Numerator of theta
        sigma_absolute = abs(m1(i))+ abs (m2(i) ); % Denominator of theta
        theta = sigma_macaulay / sigma_absolute ; % Calculation of theta
        radio (i) =((1) /( theta +((1 - theta ) /(n)) )) *(q/ sqrt ([ m1(i) m2(i) 0 nu *( m1(i)+m2(i)) ]*...
            ce_inv *[ m1(i) m2(i) 0 nu *( m1(i) +m2(i)) ]'));
        s1(i)=radio(i)*m1(i);
        s2(i)=radio(i)*m2(i);
    end
    hplot =plot(s1,s2,tipo_linea);
end

```

### B.1 Rate dependent model / viscous model

```

% following a re the changes made in rmap_dano1.m
if(rtrial > r_n)
    %* Loading
    fload=1;
    if Eprop (6) ==1 && MDtype ==1 % Viscous case and symmetric model
        r_n1 =((eta-delta_t*(1 - alpha ))*r_n+( delta_t*rtrial ) ) /( eta+alpha*delta_t );
    else
        r_n1 = rtrial;
    end
end

```

```

% following are the changes made in damage_main file.
]for iload = 1:length(istep)
    % Load states
]    for iloc = 1:istep(iload)
        i = i + 1 ;

        TIMEVECTOR(i) = TIMEVECTOR(i-1)+ delta_t(iload) ;
        % Total strain at step "i"
        % -----
        if i >1
            eps_n = strain (i-1 ,:) ; % Use the default value
        else
            eps_n = 0; % Intialize to 0
        end
    end
end

```

```

% following are the changes made in Modelos_de_dano1.m
if Eprop(6) ==1

    alpha = Eprop(8) ;

    if ( MDtype ==1) % Symmetric case
        rtrial_n = sqrt ( eps_n *ce*eps_n' ) ;
        rtrial_n1 = sqrt ( eps_n1 *ce* eps_n1' ) ;
        rtrial =(1 - alpha )* rtrial_n + alpha * rtrial_n1 ;
    end
end

```

## B.2 Implementation of consistent tangent operator

```

function [C_alg,C_tangent] = material_matrix_upd(eps_n1,Eprop,dano_n1,ce,delt,aux_var,alpha)

eta = Eprop(7);
C_tangent =(1.d0 - dano_n1 )*ce;
Tau_n1 = sqrt ( eps_n1*ce* eps_n1' );
sigma =ce*eps_n1';
if Eprop(6) == 1
    C_alg = C_tangent - (alpha*delt)/(eta+alpha*delt ) *aux_var/Tau_n1*(sigma*sigma') ;
else
    C_alg = C_tangent - (aux_var/Tau_n1)*sigma*sigma';
end
end

```